Implications of Nonperturbative Effects for Colored Dark Sectors

Mathias Becker,[1,2] Emanuele Copello,[1,2] Julia Harz,[1,2] Kirtimaan A. Mohan,[3] and Dipan Sengupta[4]

[1]*Johannes Gutenberg Universität Mainz, Staudingerweg 9, 55128 Mainz, Germany*

[2]*Technische Universität München, James-Franck-Straße 1, 85748 Garching, Germany*

[3]*Department of Physics and Astronomy, 567 Wilson Road, East Lansing, Michigan 48824, USA*

[4]*ARC Centre of Excellence for Dark Matter Particle Physics, Department of Physics, University of Adelaide, South Australia 5005, Australia*

Abstract

The non-observation of WIMP dark matter might be explained by the existence of complex dark sectors. We illustrate, on a model of colored coannihilation, that the Sommerfeld effect and bound state formation are fundamental in calculating the relic density of dark matter accurately. We point out that a flat correction factor accounting for those effects cannot be employed. Furthermore, we find that the parameter previously excluded by experiments still remains viable. Lastly, we demonstrate that bound state searches at the LHC can be crucial in testing such a model.

1. INTRODUCTION AND MODEL

The weakly interacting massive particle (WIMP) has been an intriguing dark matter (DM) candidate for the past decades. However, its simplest realization in the form of a single component dark sector is strongly challenged by experiments. A more complex dark sector, for instance, in the form of an additional dark sector particle, can explain the non-observation of WIMP DM at direct detection experiments. An example of this is the currently widely studied model of simplified t-channel dark matter with a colored mediator [1, 2]. The colored annihilations in the dark sector can efficiently deplete the dark matter relic density given that the colored mediator is close in mass to the dark matter candidate itself. In earlier works [3], it was pointed out that colored annihilations are subject to nonperturbative effects, namely, the Sommerfeld effect (SE) and bound state formation (BSF). We demonstrate [4] the importance of the SE and BSF on a realistic model of DM by firstly determining their effect on the dark matter relic density, secondly, studying their implications on the excluded parameter space of the model, and finally exemplifying the unique constraints arising from bound state searches at the LHC.

We choose the model S3M-uR [5] as an exemplary model where the dark sector consisting of a Majorana fermion DM candidate χ and three copies of scalars X_i (coming with the quantum numbers of up-type right-handed SM quarks) interacts with the SM via

$$\mathcal{L} \supset g_{\mathrm{DM},ij} X_i^\dagger \bar{\chi} P_R q_j + h.c. \tag{1}$$

We consider the scalars to be degenerate in mass $m_{X_i} = m_X$ and to couple diagonally and democratically to the SM $g_{\mathrm{DM},ij} = g_{\mathrm{DM}}$. The dark sector is stabilized by a $\mathcal{Z}_2$ symmetry such that the lightest particle in the dark sector is stable. Thus, the relevant new parameters are the mass of the DM candidate m_χ, the mass splitting in the dark sector $\Delta m = m_X - m_\chi > 0$, and the DM-SM coupling g_{DM}.

If the portal coupling g_{DM} is large enough to equilibrate the dark sector and the SM, the time evolution of the DM density is governed by a single Boltzmann equation. The dynamics of this equation are set by an effective annihilation cross section involving a sum of all annihilations that can take place in the dark sector

$$\langle \sigma_{\mathrm{eff}} v_{\mathrm{rel}} \rangle = \sum_{ij} \langle \sigma_{ij} v_{ij} \rangle \frac{Y_i^{\mathrm{eq}} Y_j^{\mathrm{eq}}}{\tilde{Y}^{\mathrm{eq}} \tilde{Y}^{\mathrm{eq}}}. \tag{2}$$

Here, $Y_i^{\mathrm{eq}} = \frac{n_i}{s}$ is the number density divided by the entropy density of the particle species i in thermal equilibrium and $\tilde{Y} = \sum_i Y_i$. Inspecting equation (2) reveals that annihilations of the colored scalars $X_i X_j \to SM$ can dominate the effective annihilation cross section as long as the mass splitting Δm is small compared to the dark matter mass m_χ. As the scalars carry a color charge, they generate a color potential which is felt by the annihilation partner and thus can alter the result of the annihilation cross section significantly.

2. SOMMERFELD EFFECT AND BOUND STATE FORMATION AND ITS IMPLICATIONS FOR PHENOMENOLOGY

The color potential between two colored scalars X_i is generated by multiple t-channel gluon exchanges. Each gluon exchange parametrically contributes with a factor of $\frac{\alpha_s}{v}$, if $\alpha_s \sim v$. Since $\alpha_s \approx 0.1$, it is of an order of the relative velocity between the two annihilating particles, as the dark sector particles are nonrelativistic during thermal freeze-out. This implies that an $n + 1$-gluon exchange diagram cannot be omitted if an n-gluon exchange diagram is included, which indicates the need to resume these types of diagrams. In the nonrelativistic limit, this resummation simplifies to the Schrödinger equation involving a color potential [6]. As the gluons are massless, we find a Coulomb potential. Depending on the representation of the particles involved, the resulting potential can be attractive or repulsive and vary in strength. For instance, for particles in the fundamental representation of $SU(3)_C$, we find $\mathbf{3} \otimes \bar{\mathbf{3}} = \mathbf{1} \oplus \mathbf{8}$ and $\mathbf{3} \otimes \mathbf{3} = \bar{\mathbf{3}} \oplus \mathbf{6}$. The singlet $\mathbf{1}$ and the antifundamental $\bar{\mathbf{3}}$ lead to an attractive potential, while the remaining two generate a repulsive potential.

When solving the Schrödinger equation, we find solutions with positive energy eigenvalues (scattering states) and so-

lutions with negative energy eigenvalues (bound states). The scattering states lead to the Sommerfeld effect (SE), while the bound states give rise to the process of bound state formation (BSF).

2.1. Sommerfeld Effect

Scattering states are typically included when calculating the effective annihilation cross section in equation (2). However, they are modeled by plane waves, which is not a good approximation in the presence of a long-range potential, such as the Coulomb color potential. Instead of plane waves, we use the solution of the Schrödinger equation for the scattering states when calculating the effective annihilation cross section. The deviation from the result using plane waves is called the SE. The cross section is modified by a factor larger than 1 for an attractive potential, whereas it is corrected by a positive factor smaller than 1 for a repulsive one.

If the cross section is increased or decreased by the SE depends on the matrix element of the annihilation and its color decomposition and has to be calculated for each annihilation channel. We find that for parameter points where the portal coupling dominates the annihilation ($g_{DM} \gg g_s$), the SE tends to reduce the cross section. For the opposite case, $g_{DM} \ll g_s$, the SE increases the effective annihilation cross section.

2.2. Bound State Formation

Radiative BSF, $XX^\dagger \to \mathcal{B}\left(XX^\dagger\right) g$, is typically not considered in the calculation of the DM relic density. However, it can effectively contribute to dark sector annihilations, given that the formed bound state decays into SM particles rather than being ionized by gluons. All of these processes are mediated by the strong gauge coupling g_s. Therefore, BSF is negligible if the annihilations are dominated by the portal coupling $g_{DM} \gg g_s$. On the other hand, we find that BSF dominates the annihilation if $g_{DM} \ll g_s$. The effects of SE and BSF in the different regimes are summarized in Table 1.

Note that the effects vary in size and sign over the two regimes and thus can not be incorporated by means of a flat factor and need to be calculated for each parameter point via

$$\langle \sigma_{\text{eff}} v \rangle = \sum_{i,j} \left\langle S\left(\alpha/v_{ij}\right) \cdot \sigma_{ij} v_{ij} \right\rangle \frac{n_i^{\text{eq}}}{n^{\text{eq}}} \frac{n_j^{\text{eq}}}{n^{\text{eq}}} + \langle \sigma_{\text{BSF}} v \rangle_{\text{eff}} \left(\frac{n_X^{\text{eq}}}{n^{\text{eq}}}\right)^2 .$$
(3)

Here, $S(\alpha/v_{ij})$ is the Sommerfeld factor and $\langle \sigma_{\text{BSF}} v \rangle_{\text{eff}}$ is the effective BSF cross section, where the subscript effective accounts for the ratio of bound states decay into SM particles before being ionized.

2.3. Phenomenological Implications

When constraining this model of freeze-out DM, we determine the smallest value of the portal coupling g_{DM} for each mass structure $(m_\chi, \Delta m)$ such that DM is not overproduced. Subsequently, we check if this lower bound on g_{DM} contradicts the upper bounds arising from direct detection experiments or prompt collider searches. If the bounds are in conflict with each other, we consider the parameter point $(m_\chi, \Delta m)$ to be excluded by the experiment. Since the SE and BSF alter the calculation of the effective annihilation cross section (see equation (3)), the lower bound on g_{DM} changes accordingly. In Figure 1, we show

$\langle \sigma_{\text{eff}} v \rangle$	Sommerfeld effect	Bound state formation
$g_{DM} \gg g_s$	−	0
$g_{DM} \ll g_s$	+	++

TABLE 1: The effects of the SE and BSF on the effective annihilation cross section are summarized for the regimes of the portal couplings domination and strong gauge coupling domination. A + indicates an enhancement of the cross section, a − a reduction, a ++ a very large enhancement, and a 0 implies that the effect is negligible.

limits on the model described above arising from XENON1T, Pico-60, and LHC results at 139 fb^{-1} and 37 fb^{-1}.

The constraints are displayed in the plane spanned by the DM mass m_χ and the mass splitting Δm. The coupling g_{DM} at each point $(m_\chi, \Delta m)$ is fixed to the smallest value that does not overproduce DM. We observe significant changes in the exclusion limits depending on the contributions considered for the calculation of the relic density. The masses displayed, besides in the upper-right corner, fall into a regime where the strong gauge coupling tends to dominate the annihilation, i.e., $g_s \gtrsim g_{DM}$. As discussed earlier, and illustrated in Table 1, in this regime, the SE and especially BSF significantly enhance the annihilation cross section. Thus, the lower bound on the coupling g_{DM} arising from the relic density is lowered and, in return, experimental constraints from prompt collider searches and direct detection experiments are lifted.

In Figure 1, this effect is clearly visible in the regions where the model can produce the observed relic density and is not in contradiction with any experiment (white regions) open up. In particular, the unconstrained area between the limits from XENON1T (green) and the gray region, in which DM is always underproduced via thermal freeze-out,[1] is enlarged significantly, while a purely perturbative calculation obtains a maximal DM mass of $m_\chi \lesssim 1$ TeV in this region, including the SE that already leads to a relaxed bound of $m_\chi \lesssim 1.4$ TeV. The full calculation including the SE and BSF arrives at an upper limit of $m_\chi \lesssim 2.4$ TeV, which is a 140% correction on the limit obtained in the purely perturbative calculation. Furthermore, the viable mass splittings in this region shift from $\Delta m \lesssim 30$ GeV in a perturbative calculation to $\Delta m \lesssim 50$ GeV considering the SE and BSF.

We conclude that nonperturbative effects induce a significant shift in the exclusion limits in the strongly coannihilating regime ($\Delta m \ll m_\chi$) and cannot be neglected. Moreover, it is not sufficient to only consider the SE since the most sizable contribution arises from BSF.

2.4. Bound State Formation at the LHC

Lastly, we would like to comment on the limits arising from bound state searches at the LHC, displayed in cyan within Figure 1. At the LHC, the leading order production cross section for the bound state $\mathcal{B}(XX^\dagger)$ in the narrow width approxima-

---

[1]Note that while all other thoroughly colored areas display strict exclusion limits, the gray area only indicates where DM freeze-out does not suffice to produce all of the observed DM relic density. In this sense, the model is not strictly excluded but would require an additional DM component or an alternative production mechanism, such as freeze-in or conversion-driven freeze-out [7], in this region.
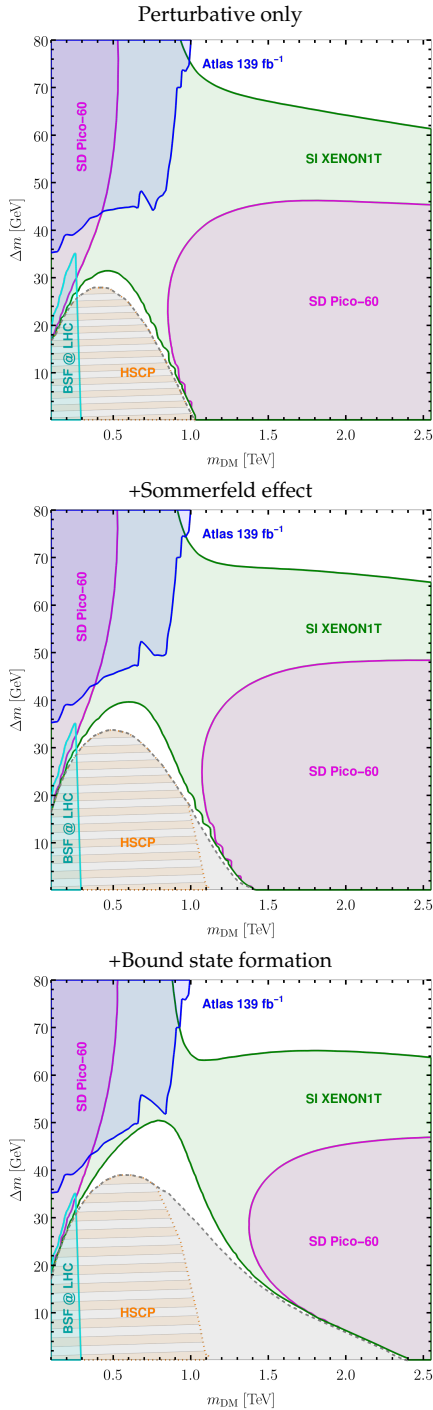
FIGURE 1: Exclusion limits on the model are shown for a calculation of the relic density including perturbative contributions only, including the SE, and complete calculation including the SE and BSF. Regions colored in green (magenta, blue, cyan) indicate parameter points which are excluded by direct detection (indirect detection, prompt collider searches, bound state searches at the LHC). Within the gray region, DM is always underproduced via thermal freeze-out. The orange-shaded region illustrates an estimate for the potential of long-lived-particle searches to constrain out-of-equilibrium production of DM, which can produce the observed relic density in the gray region. The figure is taken from [4].

tion is given by [8]

$$
\sigma \left(pp \to \mathcal{B} \left(XX^\dagger \right) \right)
$$
$$
= \frac{\pi^2}{8m_\mathcal{B}^3} \Gamma \left(\mathcal{B} \left(XX^\dagger \right) \to gg \right) \mathcal{P}_{gg} \left(\frac{m_\mathcal{B}}{13\,\mathrm{TeV}} \right), \tag{4}
$$

where $m_\mathcal{B}$ is the mass of the bound state, $\mathcal{P}_{gg}\left(\frac{m_\mathcal{B}}{13\,\mathrm{TeV}}\right)$ is the gluon-gluon luminosity for proton-proton collisions at 13 TeV, and $\Gamma(\mathcal{B}(XX^\dagger) \to gg)$ is the decay width of the bound state into a pair of gluons. Note that this formula is only valid if the total decay width of the bound state $\Gamma_\mathcal{B}$ is smaller than the binding energy E_B. For $E_B \gtrsim \Gamma_\mathcal{B}$, the production cross section for bound states is significantly suppressed compared to equation (4). As long as $g_{\mathrm{DM}} \lesssim g_s \sim 1$, the decay width of the bound states is dominated by the decay into a pair of gauge bosons, and we find $\Gamma_\mathcal{B} \lesssim E_B$, whereas for $g_{\mathrm{DM}} > g_s$ the narrow width approximation can be violated and the production of bound states at the LHC becomes irrelevant.

Inspecting the production cross section in equation 4 reveals that the production of bound states as well as the subsequent decay into a detectable pair of gauge bosons only depend on gauge couplings and are independent of the portal coupling g_{DM} as long as $g_{\mathrm{DM}} \lesssim g_s$, implying that constraints from bound state searches probe all couplings $g_{\mathrm{DM}} \lesssim g_s$. This feature differs from prompt or long-lived particle searches which rely on a large coupling g_{DM} for a prompt decay or a very small coupling for a collider stable particle or displaced vertex. In this sense, bound state searches at the LHC can provide a bridge between those two types of searches as we illustrate in Figure 2.

Current limits for stoponium-like bound states from 37 fb^{-1} data constrain mediator masses $m_X \lesssim 290$ GeV, as illustrated in Figure 1. Remarkably, they are the only limits that strictly exclude parameter space in the gray area, where DM is underproduced by DM freeze-out. We expect rescaled projected limits for the HL-LHC at 300 fb^{-1} to result in constraints of $m_X \lesssim 650$ GeV.

3. CONCLUSION

We have investigated the impact of nonperturbative effects, namely, the Sommerfeld Effect (SE) and bound state formation (BSF), arising from long-range forces in the dark sector between colored mediators. As an example, we choose a model of simplified t-channel DM, where the dark sector consists of a Majorana DM fermion χ and three colored scalars X_i with the quantum numbers of an up-type right-handed quark. If the dark sector particles are close in mass, the DM annihilation cross section can be dominated by the annihilations of X and the SE and BSF are an unavoidable consequence of the color charge present in the dark sector and thus need to be included.

We have shown that the SE and BSF cannot be accounted for by means of a flat correction factor as they not only vary significantly in their size but also can enhance or diminish the annihilation cross section of DM. Thus, the SE and BSF have to be evaluated for each parameter point individually.

Furthermore, the exclusion limits in the strongly coannihilating regime are greatly impacted, and we observe a shift in them from $(m_\chi, \Delta m) \lesssim (1\,\mathrm{TeV}, 30\,\mathrm{GeV})$ for a purely perturbative calculation to $(m_\chi, \Delta m) \lesssim (1.4\,\mathrm{TeV}, 40\,\mathrm{GeV})$ when including the SE to $(m_\chi, \Delta m) \lesssim (2.4\,\mathrm{TeV}, 50\,\mathrm{GeV})$ when including both the SE and BSF. Thus, we conclude that nonperturbative

FIGURE 2: Conceptual comparison of the constraints on the portal coupling g_{DM} arising from the three different types of searches applied in this work.

effects are fundamental when deriving exclusion limits for a model featuring a dark sector with a long-range force.

Lastly, we illustrated that bound state searches at the LHC offer a unique opportunity to constrain a wide range of couplings currently unconstrained by other prompt and long-lived collider searches. Since the bound state decay does not rely on the decay of a single particle but instead is triggered by an annihilation of the constituents, which is mediated by gauge interactions, the limits are mostly independent of the portal coupling.

CONFLICTS OF INTEREST

The authors declare that there are no conflicts of interest regarding the publication of this paper.

ACKNOWLEDGMENTS

References

[1] C. Arina, B. Fuks, L. Mantani, H. Mies, L. Panizzi, and J. Salko, "Closing in on *t*-channel simplified dark matter models," Phys. Lett. B **813** (2021), 136038 doi:10.1016/j.physletb.2020.136038 [arXiv:2010.07559 [hep-ph]].

[2] K. A. Mohan, D. Sengupta, T. M. P. Tait, B. Yan, and C. P. Yuan, "Direct detection and LHC constraints on a *t*-channel simplified model of Majorana dark matter at one loop," JHEP **05** (2019), 115 doi:10.1007/JHEP05(2019)115 [arXiv:1903.05650 [hep-ph]].

[3] J. Harz and K. Petraki, "Radiative bound-state formation in unbroken perturbative non-Abelian theories and implications for dark matter," JHEP **07** (2018), 096 doi:10.1007/JHEP07(2018)096 [arXiv:1805.01200 [hep-ph]].

[4] M. Becker, E. Copello, J. Harz, K. A. Mohan, and D. Sengupta, "Impact of Sommerfeld effect and bound state formation in simplified t-channel dark matter models," JHEP **08** (2022), 145 doi:10.1007/JHEP08(2022)145 [arXiv:2203.04326 [hep-ph]].

[5] C. Arina, B. Fuks, and L. Mantani, "A universal framework for t-channel dark matter models," Eur. Phys. J. C **80** (2020) no.5, 409 doi:10.1140/epjc/s10052-020-7933-7 [arXiv:2001.05024 [hep-ph]].

[6] K. Petraki, M. Postma, and M. Wiechers, JHEP **06** (2015), 128 doi:10.1007/JHEP06(2015)128 [arXiv:1505.00109 [hep-ph]].

[7] M. Garny and J. Heisig, "Bound-state effects on dark matter coannihilation: Pushing the boundaries of conversion-driven freeze-out," Phys. Rev. D **105** (2022) no.5, 055004 doi:10.1103/PhysRevD.105.055004 [arXiv:2112.01499 [hep-ph]].

[8] S. P. Martin, "Diphoton decays of stoponium at the Large Hadron Collider," Phys. Rev. D **77** (2008), 075002 doi:10.1103/PhysRevD.77.075002 [arXiv:0801.0237 [hep-ph]].